

## Size Effect in the (PrF<sub>3</sub> Nanoparticles—<sup>3</sup>He) System

E. M. Alakshin, R. R. Gazizulin, A. V. Klochkov, S. L. Korableva, V. V. Kuzmin,  
A. M. Sabitova, T. R. Safin, K. R. Safullin, and M. S. Tagirov

*Institute of Physics, Kazan Federal University, Kazan, 420008 Russia*

*e-mail: alakshin@gmail.com*

Received February 20, 2013; in final form, April 3, 2013

Spin kinetics of adsorbed and liquid <sup>3</sup>He in contact with crystalline nanopowders of the Van Vleck paramagnet PrF<sub>3</sub> at a temperature of 1.5 K has been studied by nuclear magnetic resonance. The correlation between the parameters of the nuclear magnetic relaxation of <sup>3</sup>He and the sizes of the sample particles has been found. A qualitative model of the magnetic relaxation of <sup>3</sup>He describing the experimental results has been proposed.

DOI: 10.1134/S0021364013100020

Hyperpolarized <sup>3</sup>He gas is widely used in neutron accelerators for the polarization of neutron beams [1–4], nuclear magnetic resonance tomography, and diverse fundamental scientific studies [5–10]. Therefore, obtaining the hyperpolarized spin state of <sup>3</sup>He nuclei using new methods remains a topical problem to date. A system consisting of PrF<sub>3</sub> Van Vleck paramagnet and <sup>3</sup>He is interesting because of the magnetic coupling between the nuclear spins of <sup>141</sup>Pr and <sup>3</sup>He found earlier [11] between the nuclei of liquid <sup>3</sup>He and crystalline PrF<sub>3</sub> powder (the particle size of 10–45 μm). The transition from the PrF<sub>3</sub> micropowders to nanopowders should increase the efficiency of the cross relaxation processes at the liquid <sup>3</sup>He–solid-state substrate interface owing to a significant increase in the surface area. Moreover, the decrease in the sample particles to nanosizes may lead to the creation of a strongly correlated spin system PrF<sub>3</sub>–<sup>3</sup>He owing to the decrease in the time of the spin diffusion over the crystal lattice and the establishment of a common spin temperature in the system during the experiment.

The nanosize PrF<sub>3</sub> samples used in this work were synthesized earlier; the stages of their synthesis by colloid chemistry were described in detail in [12–15]. The size distribution of the particles was presented. The samples were studied by X-ray analysis, nuclear pseudoquadrupole resonance, and nuclear magnetic resonance (NMR). In particular, water clusters were found in nanosize PrF<sub>3</sub> samples. Their size was determined by NMR cryoporometry and high-resolution transmission microscopy [15]. The <sup>141</sup>Pr nuclear pseudoquadrupole resonance was observed for the first time. The parameters of the nuclear spin Hamiltonian were determined. It was found that the parameters of

the crystal electric field in nanocrystals and microcrystals differ considerably [14].

In this work, the spin kinetics of adsorbed and liquid <sup>3</sup>He in contact with nanosize crystalline PrF<sub>3</sub> powders with the particle sizes of 21 ± 9 nm (sample 1) and 31 ± 10 nm (sample 2) was studied at the temperature of 1.5 K by nuclear magnetic resonance. A homebuilt pulse nuclear magnetic resonance spectrometer with the working frequency range of 3–25 MHz was used to measure the parameters of the <sup>3</sup>He nuclear magnetic relaxation. The spin–lattice relaxation times were measured by the “saturation–recovery” method with measurement of the amplitude of the free induction decay signal after the 90-degree radio-frequency pulse. The temperature of 1.5 K in the experimental cell was reached by pumping of liquid <sup>4</sup>He vapor from the cryostat.

The spin kinetics of <sup>3</sup>He in contact with sample 2 was studied in detail in [12]. A model of the longitudinal magnetization relaxation of the <sup>3</sup>He nuclei, according to which the <sup>3</sup>He relaxation takes place simultaneously through two channels, was proposed. The first channel is the relaxation of the magnetization of free <sup>3</sup>He nuclei (liquid and gaseous) via the adsorbed <sup>3</sup>He layer. The <sup>3</sup>He relaxation in the adsorbed layer is provided by the Cowan mechanism [16–19]. The second (high-field) channel of the <sup>3</sup>He relaxation is associated with the motion of <sup>3</sup>He in the quasi-periodic magnetic field owing to the anisotropy of the magnetization of separate particles of the sample of the Van Vleck PrF<sub>3</sub> paramagnet (Fatkullin mechanism) [20]. Thus, the experimental dependences of the relaxation rate of the longitudinal magnetization

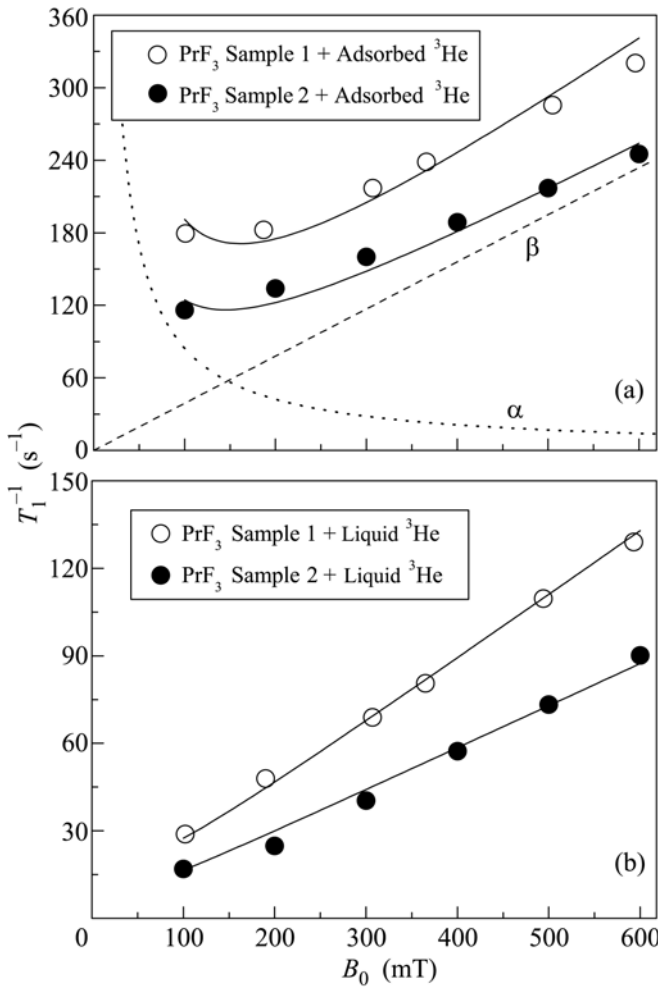


**Fig. 1.** Magnetic-field dependence of the relaxation rate of the longitudinal magnetization of the <sup>3</sup>He nuclei in the systems (a) PrF<sub>3</sub>-adsorbed <sup>3</sup>He and (b) PrF<sub>3</sub>-liquid <sup>3</sup>He for samples (open symbols) 1 and (closed symbols) 2 at a temperature of 1.5 K. Solid lines are approximations of the experimental data by formula (1). Dashed and dotted lines are decomposition of the experimental data for sample 2 into the relaxation mechanisms.

of the <sup>3</sup>He nuclei were approximated by the formula [12]

$$\frac{1}{T_1} = \frac{\alpha}{B_0} + \beta B_0, \quad (1)$$

where the first term is responsible for the relaxation channel via the adsorbed layer and the second term describes the relaxation channel owing to the motion in the inhomogeneous magnetic field.

Figure 1 shows the experimental dependences of the relaxation rate of the longitudinal magnetization of the <sup>3</sup>He nuclei in the systems PrF<sub>3</sub>-adsorbed <sup>3</sup>He and PrF<sub>3</sub>-liquid <sup>3</sup>He on the magnetic field for samples 1 and 2 at a temperature of 1.5 K (the amount of <sup>3</sup>He necessary for filling the adsorbed layer was chosen

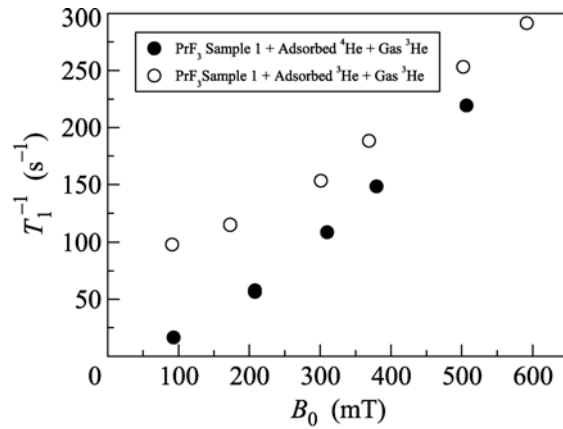


**Fig. 2.** Magnetic-field dependence of the relaxation rate of the longitudinal magnetization of the <sup>3</sup>He nuclei in the systems (open symbols) PrF<sub>3</sub>-adsorbed <sup>3</sup>He-<sup>3</sup>He gas and (closed symbols) PrF<sub>3</sub>-adsorbed <sup>4</sup>He-<sup>3</sup>He gas for sample 1 at a temperature of 1.5 K.

according to the method described in [21, 22]; in the case of liquid <sup>3</sup>He, the cell with the sample was filled completely).

To confirm the relaxation channels of the longitudinal magnetization of <sup>3</sup>He nuclei in contact with the nanosize samples of the Van Vleck paramagnet PrF<sub>3</sub> proposed earlier, experiments were performed with the samples, the surface of which was preliminarily coated with an adsorbed <sup>4</sup>He layer. The experimental dependences of the relaxation rate of the longitudinal magnetization of <sup>3</sup>He nuclei in the systems PrF<sub>3</sub>-adsorbed <sup>3</sup>He + <sup>3</sup>He gas and PrF<sub>3</sub>-adsorbed nonmagnetic <sup>4</sup>He isotope + <sup>3</sup>He gas on the magnetic field for sample 1 at a temperature of 1.5 K are shown in Fig. 2. It can be seen that, when the sample surface is coated with the adsorbed layer of nonmagnetic <sup>4</sup>He, the low-field relaxation channel owing to the adsorbed film disappears completely, while the high-field channel remains almost unchanged.

Approximations of the experimental data by formula (1) for samples 1 and 2 are shown by solid lines in Fig. 1a, where the dashed and dotted lines are the decomposition into two relaxation channels for sample 2. The weight coefficients  $\alpha$  and  $\beta$  obtained from the approximation of all experimental data shown in Fig. 1 are given in the table.

The detailed consideration of the experimental dependences of the relaxation rate of the longitudinal magnetization of <sup>3</sup>He nuclei on the magnetic field in the system PrF<sub>3</sub>-liquid <sup>3</sup>He for samples 1 and 2 (Fig. 1b) vividly shows that the contribution to the relaxation from the motion of <sup>3</sup>He molecules in the periodically changing magnetic field owing to the anisotropy of the magnetization of separate sample

Parameters of approximation (1) of the experimental dependences of the relaxation rate of the longitudinal magnetization of the <sup>3</sup>He nuclei in the systems PrF<sub>3</sub>–adsorbed <sup>3</sup>He and PrF<sub>3</sub>–liquid <sup>3</sup>He on the magnetic field for samples 1 and 2

System	$\alpha$	$\beta$
PrF <sub>3</sub> sample 1 + adsorbed <sup>3</sup> He	13 800 ± 1200	0.53 ± 0.01
PrF <sub>3</sub> sample 2 + adsorbed <sup>3</sup> He	8450 ± 1000	0.39 ± 0.01
PrF <sub>3</sub> sample 1 + liquid <sup>3</sup> He	550 ± 120	0.22 ± 0.002
PrF <sub>3</sub> sample 2 + liquid <sup>3</sup> He	200 ± 40	0.145 ± 0.004

particles is dominant. The slope of these dependences differs by a factor of approximately 1.5.

The ratio of the  $\beta$  coefficients (see table) for samples 1 and 2 for the systems PrF<sub>3</sub>–adsorbed <sup>3</sup>He and PrF<sub>3</sub>–liquid <sup>3</sup>He is  $1.36 \pm 0.06$  and  $1.52 \pm 0.04$ , respectively.

Taking into account that the size of particles of sample 1 is 1.5 times less than the size of particles in sample 2, it is possible to conclude that there is a correlation between the relaxation rate of the longitudinal magnetization of the <sup>3</sup>He nuclei and the particle sizes of the samples of the Van Vleck paramagnet PrF<sub>3</sub> for the high-field relaxation channel. For completeness, it is desirable to perform experiments in a wider range of sizes of particles in the samples. However, the size of nanoparticles cannot be varied significantly with the method used to synthesize samples [12, 23].

The high-field relaxation mechanism of <sup>3</sup>He that is in contact with the nanosize PrF<sub>3</sub> samples owing to the classical diffusion motion of the <sup>3</sup>He molecules in the quasiperiodic magnetic field can be illustrated by the following model (Fig. 3). The studied samples are Van Vleck paramagnet with anisotropy of the tensor of the effective gyromagnetic ratio of the nucleus of the Van Vleck Pr<sup>3+</sup> ion (tensor components:  $\gamma_x/2\pi = 33.22$  MHz/T,  $\gamma_y/2\pi = 32.42$  MHz/T,  $\gamma_z/2\pi = 100.35$  MHz/T [24]). The particle size is tens of nanometers and the samples are not oriented in the external magnetic field. Thus, each sample particle in the magnetic field creates a local macroscopic moment collinear to the external magnetic field. Its value depends on the orientation of the nanoparticle (gyromagnetic ratio tensor). The <sup>3</sup>He molecule ( $D = 6.4 \times 10^{-5}$  cm<sup>2</sup>/s) that moves rapidly in the space between the particles undergoes the fluctuations of the magnetic field. During the experiment, the <sup>3</sup>He molecule moves in the space between hundreds of particles. The fluctuation frequency of the magnetic field increases with the external magnetic field. Accordingly, the relaxation rate of the longitudinal magnetization of the <sup>3</sup>He nuclei will increase as well. As was mentioned above, the size of particles of sample 2 is larger than that of sample 1 by a factor of 1.5. Correspondingly, the frequency of fluctuations of the magnetic field for the <sup>3</sup>He molecule moving in sample 2 is lower by a factor of 1.5. As a result, the corresponding

nuclear spin–lattice relaxation rate is lower by the same factor.

Figure 3 shows the results of the computer calculations of the simplified two-dimensional model of the classical diffusion motion of <sup>3</sup>He molecules in the program FEMM (Finite Element Method Magnetics). It shows the nanoparticles of the same size in the hexa-

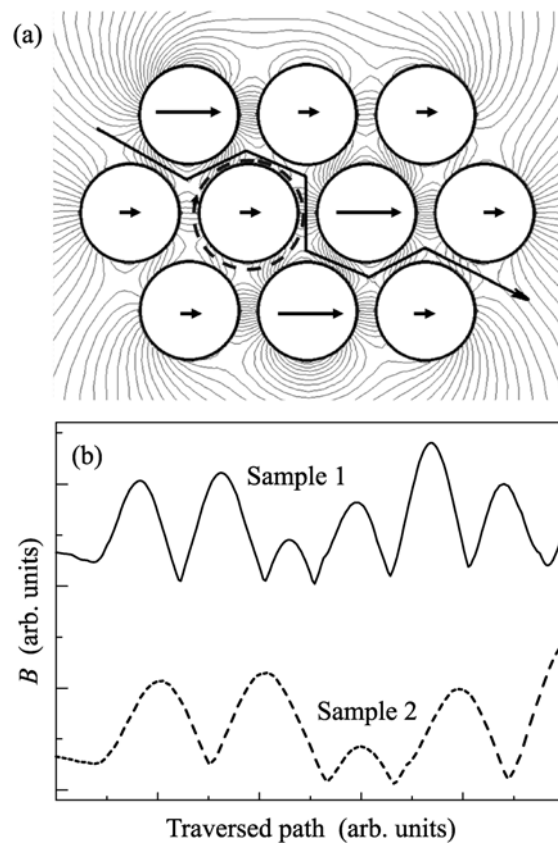


**Fig. 3.** (a) Results of the FEMM computer calculations of the simplified two-dimensional model of the classical diffusion motion of the <sup>3</sup>He molecules (solid line) in the space between the particles of the unoriented PrF<sub>3</sub> nanopowder and (dotted line) over the particle surface in the adsorbed layer. Arrows show the local magnetic moments of each particle of the unoriented Van Vleck sample in the external magnetic field. Calculations of the magnetic fields in the space between the particles are shown by the field lines. (b) Fluctuations of the magnetic field during the motion in the space between the particles for samples 1 and 2.

gonal close packing. Arrows show the local magnetic moments of each particle of the unoriented Van Vleck sample in the external magnetic field. The magnetic fields in the space between the particles were calculated. They are represented by the field lines in the figure. Fluctuations of the magnetic field were simulated for two paths of the motion of the  $^3\text{He}$  molecule (in the adsorbed layer and in the space between the particles). The case of the motion in the space between the particles for samples 1 and 2 is presented in Fig. 3b. It can be seen that, according to the calculation results, the fluctuation frequency of the magnetic field differs by a factor of 1.5. It should be noted that the result is the same for the  $^3\text{He}$  molecules moving in the adsorbed layer.

Thus, the correlation between the parameters of the nuclear magnetic relaxation of  $^3\text{He}$  and the sizes of the sample particles has been found in the NMR study of the spin kinetics of adsorbed and liquid  $^3\text{He}$  that is in contact with crystalline nanopowders of the Van Vleck paramagnet  $\text{PrF}_3$ . The proposed model qualitatively describes the experimental data.

We are grateful to Prof. N.F. Fatkullin for useful discussions and valuable advice. This work was partly supported by the Russian Foundation for Basic Research (project no. 12-02-97048-r\_povolzhie\_a) and the Ministry of Education and Science of the Russian Federation (project no. 02.G25.31.0029).

#### REFERENCES

1. T. R. Gentile, E. Babcock, J. A. Borchers, et al., *Phys. B: Condens. Matter* **356**, 96 (2005).
2. A. K. Petoukhov, K. H. Andersen, D. Jullien, et al., *Phys. B: Condens. Matter* **385–386**, 1146 (2006).
3. L. J. Chang, R. Mueller, S. Appelt, et al., *Phys. B: Condens. Matter* **350**, E707 (2004).
4. J. Krimmer, M. Distler, W. Heil, et al., *Nucl. Instrum. Methods Phys. Res.* **611**, 18 (2009).
5. E. J. van Beek, J. M. Wild, H.-U. Kauczor, et al., *J. Magn. Reson. Imag.* **20**, 540 (2004).
6. W. G. Schreiber, A. E. Morbach, T. Stavngaard, et al., *Respir. Physiol. Neurobiol.* **25**, 23 (2005).
7. S. Patz, I. Muradian, M. I. Hrovat, et al., *Acad. Radiol.* **15**, 713 (2008).
8. E. Baudin, M. E. Hayden, G. Tastevin, et al., *Compt. Rend. Chim.* **11**, 560 (2008).
9. R. R. Gazizulin, A. V. Klochkov, V. V. Kuzmin, et al., *Appl. Magn. Reson.* **38**, 271 (2010).
10. R. R. Gazizulin, A. V. Klochkov, V. V. Kuzmin, et al., *Magn. Reson. Solids EJ* **11** (2), 33 (2009).
11. A. V. Egorov, D. S. Irisov, A. V. Klochkov, et al., *JETP Lett.* **86**, 416 (2007).
12. M. S. Tagirov, E. M. Alakshin, R. R. Gazizulin, et al., *J. Low Temp. Phys.* **162**, 645 (2011).
13. E. M. Alakshin, B. M. Gabidullin, A. T. Gubaidullin, et al., arXiv:1104.0208 (2011).
14. E. M. Alakshin, A. S. Aleksandrov, A. V. Egorov, et al., *JETP Lett.* **94**, 259 (2011).
15. E. M. Alakshin, D. S. Blokhin, A. M. Sabitova, et al., *JETP Lett.* **96**, 194 (2012).
16. B. P. Cowan, *J. Low Temp. Phys.* **50**, 135 (1983).
17. R. C. Richardson, *Physica B* **126**, 298 (1984).
18. A. V. Klochkov, V. V. Kuzmin, K. R. Safiullin, et al., *JETP Lett.* **88**, 823 (2008).
19. A. Klochkov, V. Kuzmin, K. Safiullin, et al., *J. Phys.: Conf. Ser.* **150**, 032043 (2009).
20. N. F. Fatkullin, *JETP* **74**, 833 (1992).
21. E. M. Alakshin, R. R. Gazizulin, A. V. Klochkov, et al., *JETP Lett.* **93**, 223 (2011).
22. E. M. Alakshin, R. R. Gazizulin, A. V. Klochkov, et al., *J. Phys.: Conf. Ser.* **324**, 012028 (2011).
23. L. Ma, W. Chen, Y. Zheng, et al., *Mater. Lett.* **61**, 2765 (2007).
24. I. G. Bol'shakov and M. A. Teplov, Available from VINITI No. 1274, 79 (1979).

*Translated by L. Mosina*